Analytic approximations to the phase diagram of the Jaynes-Cummings-Hubbard model

Alexander Mering* and Michael Fleischhauer
Fachbereich Physik and Research Center OPTIMAS, Technische Universität Kaiserslautern, D-67663 Kaiserslautern, Germany

Peter A. Ivanov and Kilian Singer
Institut für Quanteninformationsverarbeitung, Universität Ulm, Albert-Einstein-Allee 11, 89081 Ulm, Germany
(Received 21 August 2009; published 16 November 2009)

We discuss analytic approximations to the ground-state phase diagram of the homogeneous Jaynes-Cummings-Hubbard (JCH) Hamiltonian with general short-range hopping. The JCH model describes, e.g., radial phonon excitations of a linear chain of ions coupled to an external laser field tuned to the red motional sideband with Coulomb-mediated hopping or an array of high-Q coupled cavities containing a two-level atom and photons. Specifically, we consider the cases of a linear array of coupled cavities and a linear ion chain. We derive approximate analytic expressions for the boundaries between Mott-insulating and superfluid phases and give explicit expressions for the critical value of the hopping amplitude within the different approximation schemes. In the case of an array of cavities, which is represented by the standard JCH model, we compare both approximations to numerical data from density-matrix renormalization-group calculations.

DOI: 10.1103/PhysRevA.80.053821 PACS number(s): 42.50.Pq, 03.67.Lx, 64.70.Tg, 67.85.Hj

I. INTRODUCTION

In recent years, there has been a growing interest in quantum optics systems as an experimental testing ground of fundamental models for quantum many-body physics and quantum simulation. The most prominent examples are certainly ultracold atoms in optical lattices [1,2], which are almost ideal representations of various types of Hubbard models [3–7]. However, due to their finite mass, atomic systems represent, with few exceptions, only models with explicit particle number conservation. On the other hand, different quantum optical systems, employing photons or quasiparticles, such as phonons, have been suggested recently, which are not limited by this constraint. For example, an array of coupled high-Q microcavities containing a two-level atom and a photon is described by the Jaynes-Cummings-Hubbard model (JCHM) [8–11]. It is a combination of two well-known systems, the Jaynes-Cummings model [12,13], describing the coupling of a single two-level system to a bosonic mode, and the hard-core Bose-Hubbard model [14], which describes the interaction and tunneling of bosons on a lattice. Recently, we have shown that a modification of the JCHM can also be implemented in a linear ion trap, which has the advantage of an easier experimental realization since the required parameter regime is already realizable with current technology [15]. A large variety of analytic and numeric methods was applied to the JCHM and related models, providing profound results for the phase diagram and other ground-state quantities [16–23]. In the present paper, we show that in the strong-interaction limit and near commensurate filling simple approximate analytic solutions of the JCHM can be found if there is translational invariance, i.e., for an infinite homogeneous system or periodic boundary conditions realizable, e.g., with ions in a race-track Paul trap design. These solutions provide a good analytic approximation to the full ground-state phase diagram.

*amering@physik.uni-kl.de

This paper is structured as follows. In Sec. II, we will briefly summarize the main properties of the Jaynes-Cummings model, together with other important quantities needed later on. In Sec. III, we introduce two different approximation schemes, both giving analytic results for the critical hopping amplitude for the Mott-insulator (MI) to superfluid (SF) transition. In Sec. IV, we apply both approximations to the simple cubic nearest-neighbor JCH model, describing an array of coupled cavities and to the special case of a linear ion chain.

II. JCH MODEL

In this section, we will shortly review the main features of the JCH model defined by the Hamiltonian

$$\hat{H} = \omega \sum_j \hat{a}_j^\dagger \hat{a}_j + \Delta \sum_j \hat{\sigma}_j^\dagger \hat{\sigma}_j^- + g \sum_j (\hat{\sigma}_j^\dagger \hat{a}_j + \hat{a}_j^\dagger \hat{\sigma}_j^-) + \sum_d t_d \sum_j (\hat{a}_j^\dagger \hat{a}_{j+d} + \hat{a}_{j+d}^\dagger \hat{a}_j) \quad (1)$$

and discuss the main quantities needed in order to calculate its phase diagram. The system (1) comprises bosonic and spin degrees of freedom, the specific interpretation of which depends on the actual physical system. Depending on the implementation, $\hat{a}_j^\dagger$ and $\hat{a}_j$ describe the creation and annihilation of a photon (phonon) at the jth cavity (ion), $\hat{\sigma}_j^\pm$ are the spin-flip operators between the internal states of the atom (ion), and Δ is the transition energy of the atom (the detuning of the external laser field from the red motional sideband). g describes the cavity-mediated atom-photon coupling (the phonon-ion coupling in the Lamb-Dicke limit) and ω is the cavity resonance (the local oscillation) frequency. Between separated cavities (ions), there is a photon (phonon) transfer described in Eq. (1) by the distance-dependent hopping amplitude t_d.

In the limit of vanishing hopping $t_d \equiv 0$, the resulting Jaynes-Cummings model can easily be diagonalized. In this

case, all sites j decouple and become independent. Since the total number of excitations $\hat{N}_j=\hat{a}_j^\dagger\hat{a}_j+\hat{\sigma}_j^+\hat{\sigma}_j^-$ on every site j is a constant of motion, the local JC Hamiltonian block diagonalizes. Within each two-dimensional excitation subspace, the eigenstates can easily be found. Adapting the notation from [18], these are given by

$$|\pm,n\rangle = \frac{[\chi_n \mp (\omega-\Delta)]|\uparrow,n-1\rangle \pm 2g\sqrt{n}|\downarrow,n\rangle}{\sqrt{2}\sqrt{\chi_n^2 \mp (\omega-\Delta)\chi_n}} \tag{2}$$

$$:= \alpha_n^\pm|\uparrow,n-1\rangle \pm \beta_n^\pm|\downarrow,n\rangle, \tag{3}$$

with $\chi_n=\sqrt{(\Delta-\omega)^2+4ng^2}$ and $n>0$, and the eigenenergies are

$$E_n^\pm = n\omega + \frac{\Delta-\omega}{2} \pm \frac{1}{2}\chi_n. \tag{4}$$

For $n=0$, the ground state is nondegenerate and given by $|-,0\rangle=|\downarrow,0\rangle$ with $E_0=0$. Here, the state $|\uparrow,n-1\rangle$ describes an atomic excitation together with $n-1$ bosonic excitations; $|\downarrow,n\rangle$ is the state with the atom in the ground state and n bosonic excitations. In the strong-interaction limit $g\gg|\Delta-\omega|$, the energy gap $\Delta E_n=E_n^+-E_n^-=\chi_n\sim 2g\sqrt{n}$ is large compared to any other energy scale in the system and, thus, the excited states $|+,n\rangle$ do not contribute to the ground state.

For the following discussion, it will be useful to consider the action of a single bosonic creation or annihilation operator on a given JC eigenstate $|\pm,n\rangle$. Defining

$$A_n^\pm = \begin{cases} \sqrt{n}\alpha_n^\pm\beta_{n+1}^- \pm \sqrt{n+1}\beta_n^\pm\alpha_{n+1}^-, & n>0, \\ \alpha_1^-, & n=0, \end{cases} \tag{5}$$

$$B_n^\pm = \begin{cases} \sqrt{n}\alpha_n^\pm\beta_{n+1}^+ \mp \sqrt{n+1}\beta_n^\pm\alpha_{n+1}^+, & n>0, \\ -\alpha_1^+, & n=0, \end{cases} \tag{6}$$

$$C_n^\pm = \begin{cases} \sqrt{n-1}\alpha_n^\pm\beta_{n-1}^- \pm \sqrt{n}\beta_n^\pm\alpha_{n-1}^-, & n>1, \\ 0, & n\le 1, \end{cases} \tag{7}$$

$$D_n^\pm = \begin{cases} \sqrt{n-1}\alpha_n^\pm\beta_{n-1}^+ \mp \sqrt{n}\beta_n^\pm\alpha_{n-1}^+, & n>1, \\ \pm\beta_1^\pm\delta_{n,1}, & n\le 1, \end{cases} \tag{8}$$

the action of $\hat{a}^\dagger$ and $\hat{a}$ on the state $|\pm,n\rangle$ can be seen to be

$$\hat{a}^\dagger|\pm,n\rangle = A_n^\pm|+,n+1\rangle + B_n^\pm|-,n+1\rangle, \tag{9}$$

$$\hat{a}|\pm,n\rangle = C_n^\pm|+,n-1\rangle + D_n^\pm|-,n-1\rangle, \tag{10}$$

i.e., $\hat{a}^\dagger$ and $\hat{a}$ connect the manifold of states $|\pm,n\rangle$ to the manifolds $|\pm,n+1\rangle$ and $n>0$, respectively, as expected.

In order to calculate the phase boundaries of the Mott-insulating lobes for the JCH model, we will follow the usual route. Since the total number of excitations in the system

$$\hat{N} = \sum_j (\hat{a}_j^\dagger\hat{a}_j + \hat{\sigma}_j^+\hat{\sigma}_j^-) \tag{11}$$

commutes with the full Hamiltonian (1), it is enough to treat the system for a fixed number of excitations. The boundary of the nth Mott lobe can then be determined by calculating the total energy $E(N)$ for $N=nL-1$, $N=nL$, and $N=nL+1$ excitations in a system with L sites. The chemical potential then reads as

$$\mu_n^\pm = \pm[E(nL\pm 1)-E(nL)], \tag{12}$$

where the plus sign belongs to the upper boundary of the Mott lobe and the minus sign to the lower one. For $t_d\equiv 0$, $\mu_n^\pm$ can be calculated straightforwardly. Starting with the energy for $N=nL$ excitations with n being an integer, i.e., for a commensurate number of excitations, it can be seen that due to the nonlinear dependence of the single-site energy E_n^- on n, the excitations will distribute equally over the whole lattice. The ground state is therefore given by $\vec{n}=\{n,n,\ldots,n\}$. Now, when adding (removing) a single excitation from the whole system, the ground state is given by $\{n\pm 1,n,\ldots,n\}$, where we have ignored the degeneracy of the state since we are only interested in the energy and the system is homogeneous. With this, the energies at $t_d=0$ can be written as

$$E(nL-1) = (L-1)E_n^- + E_{n-1}^-, \tag{13}$$

$$E(nL) = LE_n^-, \tag{14}$$

$$E(nL+1) = (L-1)E_n^- + E_{n+1}^-, \tag{15}$$

and the chemical potentials evaluate to

$$\mu_n^+ = E_{n+1}^- - E_n^- \tag{16}$$

$$= \omega - \frac{\chi_{n+1}}{2} + (1-\delta_{n0})\frac{\chi_n}{2} + \delta_{n,0}\frac{\Delta-\omega}{2}, \tag{17}$$

for any n and

$$\mu_n^- = E_n^- - E_{n-1}^- \tag{18}$$

$$= \omega - \frac{\chi_n}{2} + (1-\delta_{n1})\frac{\chi_{n-1}}{2} + \delta_{n,1}\frac{\Delta-\omega}{2}, \tag{19}$$

for $n>0$. Thus, for a commensurate number of excitations the system displays particle-hole gaps. Since $\mu_{n+1}^-=\mu_n^+$, the chemical potential for noncommensurate total number of excitations between $N=nL$ and $N=(n+1)L$ is the same, corresponding to a critical point. For nonvanishing tunneling, the critical points extend to critical regions.

The simplest numerical method to obtain a qualitative phase diagram is the so-called mean-field theory. As described, for instance, in [10,18,21,23], the mean-field theory can be implemented by introducing an order parameter Ψ, which in our case is chosen to be homogeneous and real valued. Decoupling the hopping term by using

$$\hat{a}_j^\dagger\hat{a}_l \mapsto \Psi(\hat{a}_j^\dagger + \hat{a}_l) - |\Psi|^2, \tag{20}$$

the whole JCH Hamiltonian (1) in the grand-canonical ensemble uncouples in real space with a local Hamiltonian being

$$\hat{H}^{\mathrm{MF}} = (\omega-\mu)\hat{a}^\dagger\hat{a} + (\Delta-\mu)\hat{\sigma}^+\hat{\sigma}^- + g(\hat{a}^\dagger\hat{\sigma}^- + \hat{a}\hat{\sigma}^+) - 2\tilde{J}\Psi(\hat{a}^\dagger+\hat{a}) + 2\tilde{J}|\Psi|^2. \quad (21)$$

At this point, we omitted the spatial index because the problem is purely local. The modified hopping amplitude $\tilde{J}=-\Sigma_d t_d$ gives the effective coupling within the mean-field scheme. The phase diagram is now found by diagonalizing the mean-field Hamiltonian (21) either exactly by means of perturbation theory or numerically, setting an upper bound for the maximal number of bosonic excitations in the system. The ground-state energy is then given by $\min_\Psi E[\Psi]$ and the MI is distinguished from the SF by the value of Ψ for the minimal energy. For $\Psi\equiv 0$, the system is in a MI state, for $\Psi>0$, the ground state is superfluid. This sets the point of the MI to SF transition. It should be mentioned at this point that this method gives inadequate results in one dimension ($D=1$) but is exact for $D\to\infty$. Additionally, the effective hopping $\tilde{J}$ must be larger than zero to yield useful results.

III. APPROXIMATIVE DETERMINATION OF THE PHASE BOUNDARIES

A. Effective strong-coupling model

From the discussion above, it can be seen that the phase boundaries are defined by the closure of the particle-hole gap. In the present section, we will derive effective Hamiltonians in the strong-coupling limit for the calculation of the upper and lower chemical potentials of the nth Mott lobe, allowing to calculate the particle-hole gap in first order of the hopping amplitudes t_d. To do so, we employ degenerate perturbation theory using Kato's expansion as summarized in [24] up to first order with $H_{\mathrm{eff}}=\mathcal{P}V\mathcal{P}$. This procedure is equivalent to the polariton mapping considered in [11,22]. First, we note that according to Eq. (4) the state $|+,n\rangle$ is separated by a large energy gap from the ground state $|-,n\rangle$. Thus, $|+,n\rangle$ can be completely neglected in the following as already mentioned in [11,16].

When looking for the energy of the ground state with $N=nL$, from perturbation theory, no first-order contributions are present. So, the Hilbert space per site is one dimensional, consisting of the single state $|-,n\rangle$. Thus, up to first order, the energy is given by $E(nL)=LE_n^-$. When adding an excitation, the local Hilbert space increases; now (locally), the two states $|-,n\rangle$ and $|-,n+1\rangle$ need to be taken into account. So, in this limit, the system for an additional particle can be understood as a system consisting of effective spin $\frac{1}{2}$ particles. We will identify the states $|\Uparrow\rangle$ with the state $|-,n+1\rangle$ and $|\Downarrow\rangle$ with $|-,n\rangle$. In order to derive the effective spin $\frac{1}{2}$ model, one has to look on the action of the hopping operator $\hat{a}_{j+1}^\dagger\hat{a}_j$ on the states in the Hilbert space. Using Eqs. (5)–(8) and neglecting the contributions from the states $|+,n\rangle$ and $|+,n+1\rangle$, the hopping operator $\hat{a}_{j+1}^\dagger\hat{a}_j$ acts as

$$\hat{a}_{j+1}^\dagger\hat{a}_j|\Downarrow\rangle_{j+1}|\Uparrow\rangle_j = B_n^-D_{n+1}^-|\Uparrow\rangle_{j+1}|\Downarrow\rangle_j \quad (22)$$

within the considered subspace. Therefore, by introducing spin operators $\hat{\sigma}_j^\pm$, the hopping term is equivalent to a nearest-neighbor spin-spin interaction with

$$\hat{a}_{j+1}^\dagger\hat{a}_j = B_n^-D_{n+1}^-\tilde{\sigma}_{j+1}^+\tilde{\sigma}_j^-. \quad (23)$$

Together with the energy of the system, one can thus write an effective Hamiltonian describing the upper boundary of the nth Mott lobe

$$\tilde{H} = E_n^-\sum_j\tilde{\sigma}_j^-\tilde{\sigma}_j^+ + E_{n+1}^-\sum_j\tilde{\sigma}_j^+\tilde{\sigma}_j^- + B_n^-D_{n+1}^-\sum_d t_d\sum_j(\tilde{\sigma}_{j+d}^+\tilde{\sigma}_j^- + \tilde{\sigma}_j^+\tilde{\sigma}_{j+d}^-). \quad (24)$$

This Hamiltonian is equivalent to

$$\tilde{H} = (L-1)E_n^- + E_{n+1}^- + B_n^-D_{n+1}^-\sum_d t_d\sum_j(\tilde{\sigma}_{j+d}^+\tilde{\sigma}_j^- + \tilde{\sigma}_j^+\tilde{\sigma}_{j+d}^-) \quad (25)$$

since we are at fixed magnetization with only one spin pointing upward. This Hamiltonian can be further simplified, by using a Jordan-Wigner transformation mapping the spin operators $\tilde{\sigma}_j^-$ onto fermionic operators $\hat{c}_j$ and, subsequently, performing a Fourier transformation

$$\hat{c}_j = \frac{1}{\sqrt{L}}\sum_k e^{-2\pi ikj/L}\hat{c}_k. \quad (26)$$

Then, the ground-state wave function factorizes since the Hamiltonian decouples in momentum space

$$\tilde{H} = (L-1)E_n^- + E_{n+1}^- + 2B_n^-D_{n+1}^-\sum_d t_d\sum_k\cos\left(2\pi\frac{kd}{L}\right)\hat{c}_k^\dagger\hat{c}_k. \quad (27)$$

This model is equivalent to free fermionic particles with hopping amplitudes given by t_d. In momentum space, a single fermion will occupy the mode with the lowest energy. Thus, the total energy of the single particle and therefore the total energy of an additional excitation on top of the nth Mott insulator in the JCH model is given by

$$E(nL+1) = (L-1)E_n^- + E_{n+1}^- + F_n(k'), \quad (28)$$

where

$$F_n(k) = 2B_n^-D_{n+1}^-\sum_d t_d\cos\left(2\pi\frac{kd}{L}\right), \quad (29)$$

and the momentum mode k' is chosen such that $F_n(k)|_{k'}$ is minimal. It should be mentioned that the product $B_n^-D_{n+1}^-$ is positive for any (Δ,ω,n), so the momentum mode is purely determined by the minimum of $\Sigma_d t_d\cos(2\pi\frac{kd}{L})$.

To calculate the energy for a hole in the nth Mott insulator, we follow exactly the same route. Now, the state $|\Downarrow\rangle$ is associated with $|-,n-1\rangle$ and $|\Uparrow\rangle$ with $|-,n\rangle$. The hopping operators act as

$$\hat{a}_{j+1}^\dagger\hat{a}_j|\Downarrow\rangle_{j+1}|\Uparrow\rangle_j = B_{n-1}^-D_n^-|\Uparrow\rangle_{j+1}|\Downarrow\rangle_j \quad (30)$$

and the effective Hamiltonian is given by

$$\tilde{H} = E_{n-1}^{-}\sum_j \tilde{\sigma}_j^{-}\tilde{\sigma}_j^{+} + E_n^{-}\sum_j \tilde{\sigma}_j^{+}\tilde{\sigma}_j^{-} + B_{n-1}^{-}D_n^{-}\sum_d t_d \sum_j (\tilde{\sigma}_{j+d}^{+}\tilde{\sigma}_j^{-} + \tilde{\sigma}_j^{+}\tilde{\sigma}_{j+d}^{-}). \quad (31)$$

Here the magnetization consists of one spin pointing downward. Again, after making use of a Jordan-Wigner transformation and, subsequently, a Fourier transformation, the energy of a single hole is given by

$$E(nL-1) = (L-1)E_n^{-} + E_{n-1}^{-} + F_{n-1}(k''), \quad (32)$$

where the same condition holds for k''. Now, putting the calculated energies (28) and (32) together, the chemical potentials and therefore the boundaries of the nth Mott-insulating lobe can easily be derived. They are given by

$$\mu_n^{+} = E_{n+1}^{-} - E_n^{-} + 2B_n^{-}D_{n+1}^{-}\sum_d t_d \cos\left(2\pi\frac{k'd}{L}\right), \quad (33)$$

$$\mu_n^{-} = E_n^{-} - E_{n-1}^{-} - 2B_{n-1}^{-}D_n^{-}\sum_d t_d \cos\left(2\pi\frac{k''d}{L}\right), \quad (34)$$

where k' (k'') is chosen such that $\mu_n^{+}(k')$ [$\mu_n^{-}(k'')$] is minimal (maximal). This result generalizes the findings from [16,22] to arbitrary hoppings t_d.

B. Fermion approximation

In this section, we will apply an even simpler but not that obvious approximation. When looking at the JCH Hamiltonian (1), it can be seen that all terms are quadratic. These kinds of models are in general suited for an exact solution by means of a Fourier transform. The problem at this point is, however, that the commutation relations of spin operator $\hat{\sigma}_j^{\pm}$ are not as simple as that of bosons or fermions. This limits the applicability of a Fourier transform since the operators in momentum space will not obey the same commutation relation as in real space. The usual step of a prior Jordan-Wigner transformation, transforming the spin operators to proper fermionic operators, is not applicable in this case since the interaction part is linear in the spin operators, so the Jordan-Wigner factors do not cancel out. Thus, both transformations cannot be carried out exactly without increasing the descriptional complexity of the problem. Nevertheless, the Hamiltonian can be diagonalized by a Fourier transform in an approximate way.

As said above, all modes decouple at $t_d=0$. For this reason, the spin operators are in this limit equivalent to fermionic operators. If we assume that this replacement also holds for small values of t_d, the JCH model (1) can be rewritten in a fermionic approximation

$$\hat{H} = \omega\sum_j \hat{a}_j^{\dagger}\hat{a}_j + \Delta\sum_j \hat{c}_j^{\dagger}\hat{c}_j + g\sum_j (\hat{c}_j^{\dagger}\hat{a}_j + \hat{a}_j^{\dagger}\hat{c}_j) + \sum_d t_d \sum_j (\hat{a}_j^{\dagger}\hat{a}_{j+d} + \hat{a}_{j+d}^{\dagger}\hat{a}_j). \quad (35)$$

Here the spin operators $\hat{\sigma}^{+}$ ($\hat{\sigma}^{-}$) are replaced by fermionic operators $\hat{c}^{\dagger}$ ($\hat{c}$). Within this approximation, a Fourier transform of both the bosonic and fermionic degrees of freedom can be easily accomplished via

$$\hat{a}_j = \frac{1}{\sqrt{L}}\sum_k e^{-2\pi ikj/L}\hat{a}_k, \quad (36)$$

$$\hat{c}_j = \frac{1}{\sqrt{L}}\sum_k e^{-2\pi ikj/L}\hat{c}_k. \quad (37)$$

Here $\hat{a}_k$ and $\hat{c}_k$ are operators in momentum space. Doing so, the JCH Hamiltonian transforms to that of uncoupled Jaynes-Cummings systems

$$\hat{H} = \sum_k \omega_k \hat{a}_k^{\dagger}\hat{a}_k + \Delta\sum_k \hat{c}_k^{\dagger}\hat{c}_k + g\sum_k (\hat{c}_k^{\dagger}\hat{a}_k + \hat{a}_k^{\dagger}\hat{c}_k), \quad (38)$$

with

$$\omega_k = \omega + 2\sum_d t_d \cos\left(2\pi\frac{kd}{L}\right). \quad (39)$$

The ground state in any mode is given by the Jaynes-Cummings ground state (2) with frequency ω_k. The energy of mode k with n excitations is

$$E_k^n = (1-\delta_{n0})\left[n\omega_k + \frac{\Delta-\omega_k}{2} - \frac{1}{2}\sqrt{(\Delta-\omega_k)^2 + 4ng^2}\right]. \quad (40)$$

Since the total number of excitations in the system

$$\hat{N} = \sum_j (\hat{a}_j^{\dagger}\hat{a}_j + \hat{\sigma}_j^{\dagger}\hat{\sigma}_j^{-}) \mapsto \sum_k (\hat{a}_k^{\dagger}\hat{a}_k + \hat{c}_k^{\dagger}\hat{c}_k) \quad (41)$$

commutes with the Hamiltonian (38), a common basis can be chosen. Thus, the full solution of Eq. (38) for a fixed total number of excitations $N=nL$ is given by the distribution $\vec{n} = \{n_{k_1}, n_{k_2}, \ldots\}$ of N excitations on L momentum modes with minimal energy $E_N[\vec{n}] = \Sigma_k E_k^{n_k}$ together with the constraint $\Sigma_k n_k \equiv N$. Note that the number of momentum modes L is equal to the number of sites.

When constructing the phase diagram, the energy of $N = nL-1$, $N=nL$, and $N=nL+1$ excitations needs to be calculated. In the limit of vanishing hopping ($t=0$) and for commensurate filling, i.e., $N=nL$, the distribution of occupation numbers, which has the lowest energy, is again $\vec{n} = \{n, n, \ldots, n\}$. This corresponds to a MI state with an integer number of excitations on every lattice sites. The phase is gapped with a particle-hole gap, as described in Sec. II. When t is increased, the ground state remains the same, but the gap closes and a quantum phase transition occurs from the MI to the SF phase at some critical value of t. The only remaining thing in order to calculate the chemical potentials is to find the momentum mode, where the addition (removal) of an excitation gives the maximum (minimum) reduction (increase) in the total energy. This yields

$$\mu_n^{+} = E_{k'}^{n+1} - E_{k'}^{n}, \quad (42)$$

$$\mu_n^- = E_k^n - E_k^{n-1}, \tag{43}$$

where k' (k) is chosen such that $\mu_n^+(k')$ $[\mu_n^-(k)]$ is minimal (maximal). The actual values of k and k' depend mainly on the sign of the hopping amplitudes t_d.

IV. APPLICATION TO SPECIFIC REALIZATIONS OF THE JCH MODEL

After having introduced the two approaches used in this paper, we will apply them to the case of the simple JCHM with positive effective-mass and nearest-neighbor hopping and to a modified model describing the physics of a linear ion chain. The case of the simple JCHM essentially serves as a testing ground for our approximation schemes, including a comparison of the analytic results to numerical data from density-matrix renormalization-group (DMRG) and mean-field calculations. Later on, the generalized JCHM will be treated by both approximations giving analytic results for the phase diagram in a wide range of parameters.

A. JCHM with positive effective-mass and nearest-neighbor hopping

Without loss of generality, we will specialize here on the case discussed in [20]. The Hamiltonian of the JCHM in this case is given by

$$\hat{H} = \omega \sum_j \hat{a}_j^\dagger \hat{a}_j + \Delta \sum_j \hat{\sigma}_j^\dagger \hat{\sigma}_j^- + g \sum_j (\hat{\sigma}_j^\dagger \hat{a}_j + \hat{a}_j^\dagger \hat{\sigma}_j^-) - t \sum_j (\hat{a}_j^\dagger \hat{a}_{j+1} + \hat{a}_{j+1}^\dagger \hat{a}_j), \tag{44}$$

with $\omega=\Delta$. Comparing with the Hamiltonian (1), one notes that the hopping amplitudes satisfy $t_d=-t\delta_{d1}$.

For the calculation of the chemical potentials, we first have to determine the momentum modes k' and k'', which contribute to the energy. For $\omega=\Delta$, the coefficients in Eq. (2) are $\alpha_n^\pm=\frac{1}{\sqrt{2}}=\beta_n^\pm$ and therefore

$$B_n^- = \begin{cases} \dfrac{\sqrt{n}+\sqrt{n+1}}{2} & n>0 \\ -\dfrac{1}{\sqrt{2}} & n=0 \end{cases} = D_{n+1}^-. \tag{45}$$

With this, the function $F_n(k)$ is given by

$$F_n(k) = -t \frac{(\sqrt{n}+\sqrt{n+1})^2}{2-\delta_{n,0}} \cos\left(2\pi \frac{k}{L}\right). \tag{46}$$

Both chemical potentials have its minimum (maximum) at $k=0$. Putting everything together, the phase boundaries of the nth Mott lobe, calculated using the effective strong-coupling model read as

$$\mu_n^+ = \omega - \frac{1}{2}\chi_{n+1} + \frac{1-\delta_{n0}}{2}\chi_n - t\frac{(\sqrt{n}+\sqrt{n+1})^2}{2-\delta_{n0}}, \tag{47}$$

for any n and

$$\mu_n^- = \omega - \frac{1}{2}\chi_n + \frac{1-\delta_{n1}}{2}\chi_{n-1} + t\frac{(\sqrt{n}+\sqrt{n-1})^2}{2-\delta_{n1}}, \tag{48}$$

for $n>0$. This allows for the determination of the critical hopping amplitude t_{crit}, where $\mu_n^+=\mu_n^-$, which is given by

$$t_{\mathrm{crit}}/g = 2\frac{2\sqrt{n}-\sqrt{n+1}-\sqrt{n-1}}{(\sqrt{n}+\sqrt{n+1})^2+(\sqrt{n+\delta_{n1}}+\sqrt{n-1})^2}. \tag{49}$$

Second, we apply the second approximation to this model. With the given system parameters, the momentum-dependent phonon energies from Eq. (39) are given by

$$\omega_k = \omega - 2t\cos\left(2\pi\frac{k}{L}\right) \tag{50}$$

and the energy in the kth momentum mode for a given filling n reads as [see Eq. (40)]

$$E_k^n = (1-\delta_{n0})\left[n\omega - 2nt\cos\left(2\pi\frac{k}{L}\right) + t\cos\left(2\pi\frac{k}{L}\right) - \sqrt{t^2\cos^2\left(2\pi\frac{k}{L}\right)+ng^2}\right]. \tag{51}$$

Finally, following Eqs. (42) and (43), the momentum modes k' (k), which minimize (maximize) the chemical potentials need to be found. In the present case $(t_1<0)$, these are $k'=0$ and $k=\frac{L}{2}$. Thus, the resulting chemical potentials are

$$\mu_n^+ - \omega = -2t + t\delta_{n0} - \sqrt{t^2+(n+1)g^2} + (1-\delta_{n0})\sqrt{t^2+ng^2}, \tag{52}$$

for any n and

$$\mu_n^- - \omega = 2t - t\delta_{n1} - \sqrt{t^2+ng^2} + (1-\delta_{n1})\sqrt{t^2+(n-1)g^2}, \tag{53}$$

for $n>0$. A closed form for the critical hopping can be found but is rather lengthy and will therefore be skipped.

We now compare our analytic results to various numerical calculations. Figure 1 shows both analytic approximations along with numerical data from DMRG [20] and mean-field [23] calculations, where the modified hopping amplitude in the mean-field Hamiltonian (21) evaluates as $\tilde{J}=t$. From the figure, it can be seen that the effective model gives a much better agreement with the numerical DMRG data, especially, the slopes of the lobes agree perfectly at small hopping. The fermion approximation overestimates the size of the Mott lobe. In particular, while the lower boundaries are rather well reproduced, the upper boundaries have the wrong slope. Surprisingly though the critical hopping amplitudes seem to agree better with the DMRG data than the results obtained from the effective strong-coupling Hamiltonians. Although the fermion approximation is quantitatively worse than the effective strong-coupling Hamiltonians, it provides a simple approximative solution to the JCHM beyond the mean-field level, which has the advantage of giving a closed form of the ground state.

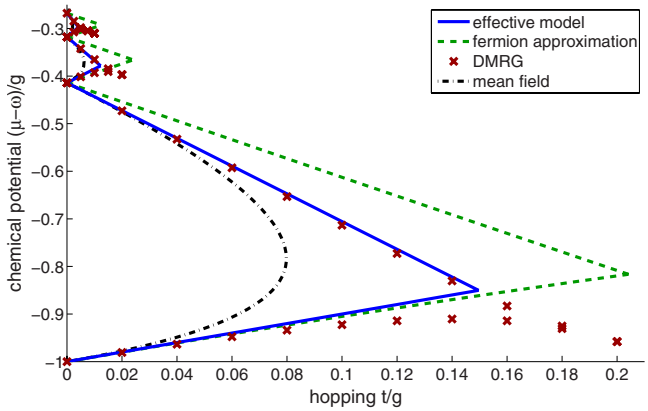

FIG. 1. (Color online) Comparison of ground-state phase diagram of the 1D JCHM (44) obtained by DMRG (data points, from [20]) as well as mean-field results (dot-dashed line) with the prediction from our approaches (solid line: strong-coupling effective Hamiltonian; dashed line: fermion approximation) for $\Delta=\omega=1$ and $g=1$. Taking into account the simplicity of both approaches, the agreement with the DMRG data is rather good while the mean-field predictions are rather poor, as expected for 1D systems. The critical hopping amplitudes estimated from the DMRG data agree surprisingly well with those predicted within the fermion approximation, although the shape of the Mott lobe is different.

B. Linear ion chain

As a second example, we consider a linear string of ions in an ion trap [15], where the ions are coupled to an external laser field and interact with each other due to the Coulomb repulsion via phonon exchange. This system is well described by a modified JCH model with a specific short-range hopping with negative effective-mass and site-dependent parameters. First, we will shortly introduce the model and give a derivation of the corresponding homogeneous limit. Afterward, we will apply the both approximations and discuss the phase boundaries within these approximations, giving explicit analytic results for them.

As shown in [15], the Hamiltonian of a linear string of L ions simultaneously irradiated by a laser, which is tuned close to the red radial motional sideband and in the Lamb-Dicke regime, is given by

$$\hat{H}=\sum_{j=0}^{L-1}\omega_j\hat{a}_j^\dagger\hat{a}_j+\Delta\sum_j\hat{\sigma}_j^\dagger\hat{\sigma}_j^-+g\sum_j(\hat{\sigma}_j^\dagger\hat{a}_j+\hat{a}_j^\dagger\hat{\sigma}_j^-)+\sum_{j=0}^{L-2}\sum_{d=1}^{L-j-1}t_{j,j+d}(\hat{a}_{j+d}^\dagger\hat{a}_j+\hat{a}_j^\dagger\hat{a}_{j+d}). \tag{54}$$

Here $\hat{a}_j^\dagger$ and $\hat{a}_j$ describe the creation and annihilation of a local phonon at the jth site (ion), $\hat{\sigma}_j^\pm$ are the spin-flip operators between the internal states of the ion, and Δ is the detuning of the external laser field from the red motional sideband. g describes the phonon-ion coupling in the Lamb-Dicke limit (for a precise definition, see [15]). The local oscillation frequencies ω_j and the hopping amplitudes $t_{j,j+d}$ are determined by the longitudinal and transversal trap frequencies ω_z and ω_x via

$$\omega_j=-\frac{\omega_z^2}{2\omega_x}\sum_{\substack{l=0\\l\neq j}}^{L-1}\frac{1}{|u_j-u_l|^3},\quad t_{j,j+d}=\frac{\omega_z^2}{2\omega_x}\frac{1}{|u_j-u_{j+d}|^3}, \tag{55}$$

where u_j are the equilibrium positions of the ions [25]. For sufficiently large L, the equilibrium positions of the ions at the center are approximately equidistant, giving $u_j=j\tilde{u}$, with $\tilde{u}$ being the distance of two adjacent ions.

Let us now discuss the limit of a homogeneous chain neglecting any boundary effect. In this limit, Eqs. (55) can be rewritten for $L\to\infty$, yielding position-independent phonon energies $\omega_j\equiv-\omega$ and hopping amplitudes $t_{j,j+d}\equiv t_d$,

$$t_d=\frac{\omega_z^2}{2\omega_x\tilde{u}^3}\frac{1}{d^3}=t\frac{1}{d^3}, \tag{56}$$

$$\omega=2\frac{\omega_z^2}{2\omega_x\tilde{u}^3}\zeta(3)=2t\zeta(3), \tag{57}$$

where $t=\frac{\omega_z^2}{2\omega_x\tilde{u}^3}$ acts as a small parameter and $\omega>0$. $\zeta(x)$ is the Riemann ζ function.

One notices a negative oscillator energy $-\omega$ and a negative effective mass, which is a result of the positive hopping strength t. This negative mass is the reason why the application of the mean-field theory is not that straight forward. When simply calculating the modified hopping amplitude $\tilde{J}=-t\Sigma_d\frac{1}{d^3}=-t\zeta(3)$, the hopping becomes negative and, therefore, the mean-field theory is inapplicable. This problem can be overcome by first applying a canonical transformation to all used operators. The transformation

$$\hat{a}_j\mapsto(-1)^j\hat{a}_j \tag{58}$$

for the annihilation operator and accordingly to all the other operators $\hat{a}_j^\dagger$, $\hat{\sigma}_j^\pm$, maps the JCH model (1) back onto itself, but with $t_d\mapsto(-1)^d t_d$. After this transformation, the modified hopping evaluates to $\tilde{J}=-t\Sigma_d\frac{(-1)^d}{d^3}=3t\zeta(3)/4$ being positive. Now the application of the mean-field theory is straightforward, following the usual route.

After having introduced the homogeneous limit of the model, the approximations introduced in Sec. III will both be applied. Starting with the effective strong-coupling theory from Sec. III A, the chemical potentials for the upper and lower boundaries of the lobes are given by Eqs. (33) and (34). The proper momentum modes k', k'', which minimize (maximize) the chemical potentials, are both found to be $k=L/2$. This results from the negative mass. Due to the complexity of the problem, especially the analytic form of B_n^- and D_n^-, analytic representation of the chemical potentials are left out here. They can be found straightforwardly just as in the case of the simple cubic JCH model.

When following the approximative method from Sec. III B, the Hamiltonian for the uncoupled JC models is given by Eq. (38), with the phonon energies being

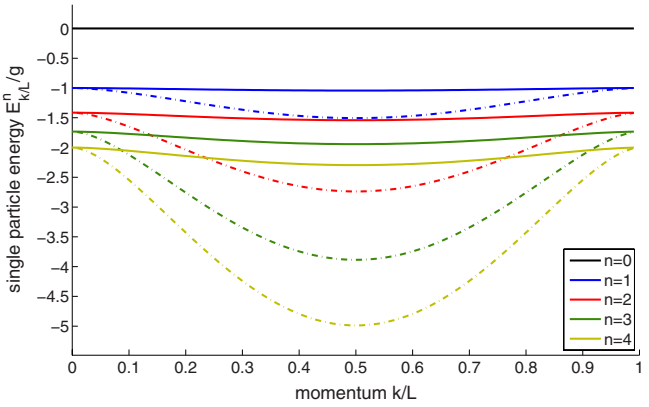

FIG. 2. (Color online) Energies of the JCH Hamiltonian for fixed filling n as function of momentum k. Shown are the energies from Eq. (4) for the five lowest fillings $0,\ldots,4$ (from top to bottom) for $\Delta=0$ and $g=1$. Solid lines: $t/g=0.02$; dashed lines: $t/g=0.2$. One clearly recognizes the minimum at $k=L/2$ and the flat dispersion for $t/g\to 0$.

$$\omega_k = -\omega + 2t\sum_d \frac{\cos\left(2\pi\frac{kd}{L}\right)}{d^3}, \tag{59}$$

according to Eq. (39). Note that since $\omega=2t\zeta(3)$, all ω_k's are negative. Using the polylogarithm $\mathrm{Li}_n(x)=\Sigma_{d=1}^{\infty}\frac{x^d}{d^n}$, one can write them in the explicit form

$$\omega_k = t[\mathrm{Li}_3(e^{2\pi ik/L}) + \mathrm{Li}_3(e^{-2\pi ik/L}) - 2\zeta(3)]. \tag{60}$$

The minimum value of $\omega_k=-7t\zeta(3)/2$ is attained for $k=\frac{L}{2}$, as expected from the positive sign of the hopping term. The energies for each momentum mode are given by the solution (40) of the JC model and the corresponding spectrum is shown in Fig. 2.

From the knowledge of the dispersion relation for different fillings, it is now easy to construct the phase diagram. As discussed in Sec. III B, the flat dispersion for $t=0$ leads to the ground state having an equal number of excitations in every momentum mode k. The chemical potentials for $t>0$ are then determined by the k' and k values, minimizing or maximizing Eqs. (42) and (43). When looking at the dispersion in Fig. 2, one recognizes that this is given for $k'=L/2$ and $k=0$. So, the chemical potentials are given by

$$\mu_n^+ = E_{L/2}^{n+1} - E_{L/2}^n, \tag{61}$$

$$\mu_n^- = E_0^n - E_0^{n-1}, \tag{62}$$

and when using the analytic form [Eqs. (40) and (60)], the phase boundaries of the nth Mott lobe read as

$$\mu_n^+ = \frac{1}{2}\Bigg\{ -\sqrt{4(n+1)g^2 + \left[\frac{7}{2}\zeta(3)t + \Delta\right]^2} - \frac{7}{1+\delta_{n0}}\zeta(3)t + \delta_{n0}\Delta + (1-\delta_{n0})\sqrt{4ng^2 + \left[\frac{7}{2}\zeta(3)t + \Delta\right]^2}\Bigg\}, \tag{63}$$

$$\mu_n^- = \frac{1-\delta_{n1}}{2}\sqrt{4(n-1)g^2+\Delta^2} - \frac{1}{2}\sqrt{4ng^2+\Delta^2} + \frac{\delta_{n1}}{2}\Delta. \tag{64}$$

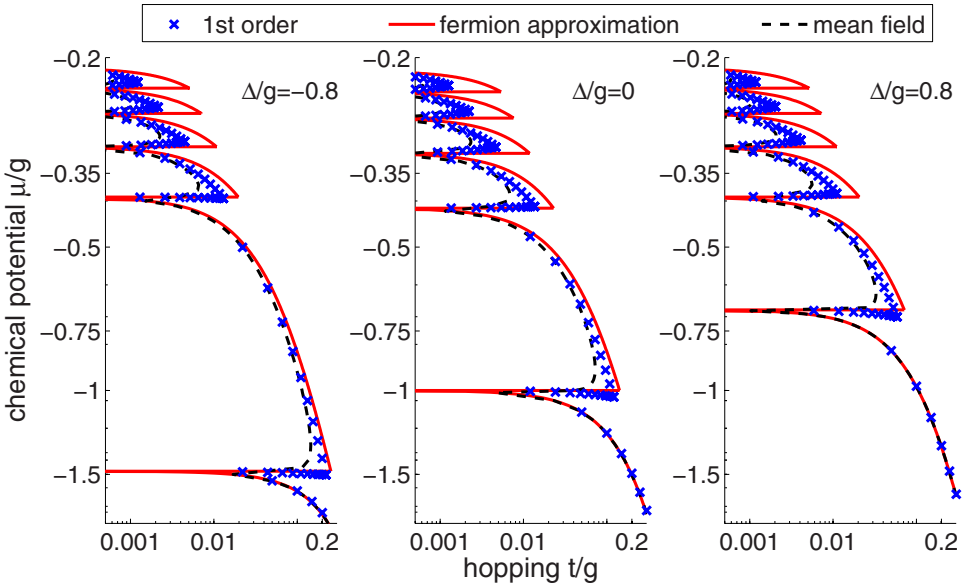

FIG. 3. (Color online) Phase diagram of the JCH model for a linear ion chain for three depicted values $\Delta/g=-0.8,0,0.8$. Shown are the upper boundary of the zero filling lobe (always lowest line) and the boundaries of the lobes with filling from 1 to 5 on a double-logarithmic scale. Beside the used approximations (solid line: fermion approximation; crosses: first-order effective theory), the results from the mean-field theory (dot-dashed line) after the canonical transformation are shown. It can be seen that the fermionic approximation again overestimates the phase boundary (compared to the more reliable effective strong-coupling theory) but gives a better agreement compared to the mean-field theory (mind the logarithmic scale).

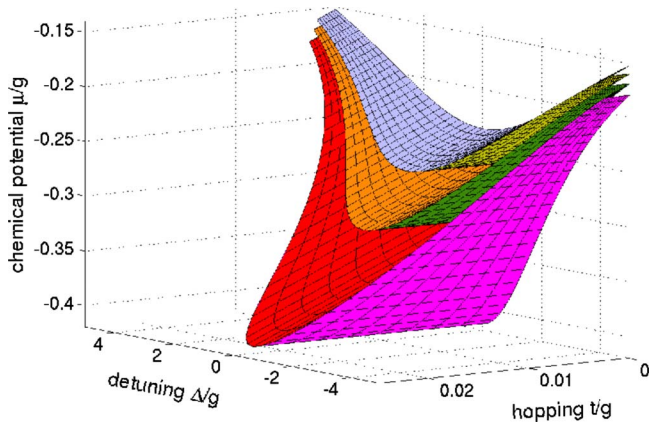

FIG. 4. (Color online) Phase diagram of the JCH model for a linear ion chain from the fermion approximation. Boundaries of the Mott-insulating lobes (from bottom to top) for $n=2,3,4$. The lobes $n=0$ and $n=1$ are not displayed since they are unbound for $\Delta \to -\infty$.

Figure 3 shows the resulting phase diagram for three values of Δ comparing the different approaches. One recognizes the typical lobe structure of the MI phases with a closing of the lobes at some value $t_n^{\mathrm{crit}}(\Delta)$. While the mean-field results underestimate the extent of the MI regions, our fermionic approach overestimates them but with a better agreement with the first-order effective strong-coupling model compared to the mean-field solution. The main advantage of the fermionic approximation is the easy closed form for the chemical potentials as well as for the ground state and a more reasonable agreement of the critical hopping amplitude $t_n^{\mathrm{crit}}(\Delta)$, as can be seen from the figure. Figure 4 shows the full phase diagram of the model as a function of the detuning Δ obtained from the fermionic approximation only.

The critical hopping amplitude $t_n^{\mathrm{crit}}(\Delta)$ can easily be calculated from the analytic expressions for the chemical potential given above. Figure 5 shows the dependence of the critical hopping amplitude from the detuning Δ for the different MI lobes. One recognizes the unboundness of the first lobe, i.e., $t_n^{\mathrm{crit}}(\Delta) \to \infty$, as $\Delta \to -\infty$.

V. SUMMARY

In summary, we have presented two simple analytic approximations to the phase diagram of the Jaynes-Cummings-Hubbard. The first approximation describes the particle-hole excitations in the vicinity of the Mott-insulator to superfluid transition for a specific filling by a simple effective spin

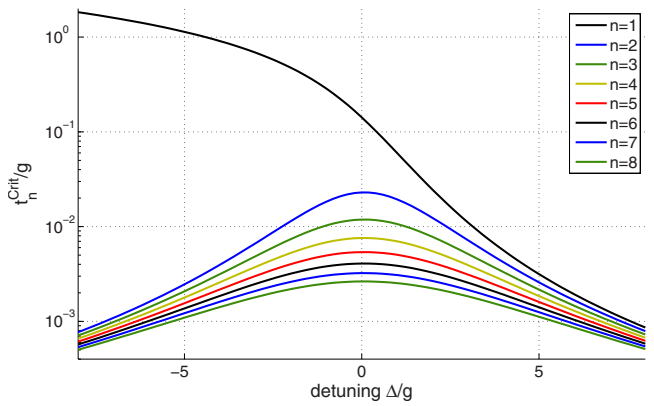

FIG. 5. (Color online) Critical hopping amplitude $t_n^{\mathrm{crit}}(\Delta)$, giving the point where the MI to superfluid transition takes place. From top to bottom: $n=1,\ldots,8$, all for $g=0.05$.

model, which generalizes the know results to arbitrary short-range hopping. The second approximation treats the spins as fermions, which allows for a simple solution of the model by means of a Fourier transformation. A comparison of both methods to DMRG and mean-field data shows reasonable agreement to the numerics. The approximative description by effective strong-coupling Hamiltonians makes very good quantitative predictions for the phase boundaries of the Mott-insulating lobes for small hopping and can be straightforwardly written down up to second order. The fermion approximation also performs very well for the lower boundaries but is less accurate for the upper ones. It does make, however, rather good predictions for the critical hopping at commensurate fillings and has the advantage of giving a closed form for the ground state in the whole parameter regime. Altogether, both methods provide quite reasonable results for the phase boundaries compared to numerical results from DMRG simulations.

ACKNOWLEDGMENTS

This work has been supported by the TMR network EMALI of the European Union and the DFG through the SFB-TR 49, the Bulgarian NSF Grants No. VU-F-205/06, No. VU-I-301/07, and No. D002-90/08, and the excellence program of the Landesstiftung Baden-Würtemberg. The authors thank E. Irish and M. Hartmann for pointing out an error in a previous version of this paper and D. Rossini and R. Fazio for providing their DMRG results shown in Fig. 1.

[1] I. Bloch, J. Dalibard, and W. Zwerger, Rev. Mod. Phys. **80**, 885 (2008).

[2] M. Greiner, O. Mandel, T. Esslinger, T. W. Hänsch, and I. Bloch, Nature (London) **415**, 39 (2002).

[3] F. H. L. Essler, H. Frahm, H. Göhmann, A. Klümper, and V. E. Korepin, *The One-Dimensional Hubbard Model* (Cambridge University Press, New York, 2008).

[4] D. Jaksch, C. Bruder, J. I. Cirac, C. W. Gardiner, and P. Zoller, Phys. Rev. Lett. **81**, 3108 (1998).

[5] A. Albus, F. Illuminati, and J. Eisert, Phys. Rev. A **68**, 023606 (2003).

[6] U. Schneider, L. Hackermüller, S. Will, T. Best, I. Bloch, T. A. Costi, R. W. Helmes, D. Rasch, and A. Rosch, Science **322**, 1520 (2008).

[7] R. Jördens, N. Strohmaier, K. Günter, H. Moritz, and T. Esslinger, Nature (London) **455**, 204 (2008).
[8] M. J. Hartmann, F. G. S. L. Brandao, and M. B. Plenio, Nat. Phys. **2**, 849 (2006).
[9] M. J. Hartmann, F. G. S. L. Brandao, and M. B. Plenio, New J. Phys. **10**, 033011 (2008).
[10] M. J. Hartmann, F. G. S. L. Brandao, and M. B. Plenio, Laser Photonics Rev. **2**, 527 (2008).
[11] D. G. Angelakis, M. F. Santos, and S. Bose, Phys. Rev. A **76**, 031805(R) (2007).
[12] E. T. Jaynes and F. W. Cummings, Proc. IEEE **51**, 89 (1963).
[13] B. W. Shore and P. L. Knight, J. Mod. Opt. **40**, 1195 (1993).
[14] M. P. A. Fisher, P. B. Weichman, G. Grinstein, and D. S. Fisher, Phys. Rev. B **40**, 546 (1989).
[15] P. A. Ivanov, S. S. Ivanov, N. V. Vitanov, A. Mering, M. Fleischhauer, and K. Singer, e-print arXiv:0905.2593v2.
[16] J. Koch and K. Le Hur, Phys. Rev. A **80**, 023811 (2009).
[17] P. Pippan, H. G. Evertz, and M. Hohenadler, Phys. Rev. A **80**, 033612 (2009).
[18] M. I. Makin, J. H. Cole, C. Tahan, L. C. L. Hollenberg, and A. D. Greentree, Phys. Rev. A **77**, 053819 (2008).
[19] M. Aichhorn, M. Hohenadler, C. Tahan, and P. B. Littlewood, Phys. Rev. Lett. **100**, 216401 (2008).
[20] D. Rossini and R. Fazio, Phys. Rev. Lett. **99**, 186401 (2007).
[21] S.-C. Lei and R.-K. Lee, Phys. Rev. A **77**, 033827 (2008).
[22] S. Schmidt and G. Blatter, Phys. Rev. Lett. **103**, 086403 (2009).
[23] A. D. Greentree, C. Tahan, J. H. Cole, and L. C. L. Hollenberg, Nat. Phys. **2**, 856 (2006).
[24] D. J. Klein, J. Chem. Phys. **61**, 786 (1974).
[25] D. F. V. James, Appl. Phys. B: Lasers Opt. **66**, 181 (1998).